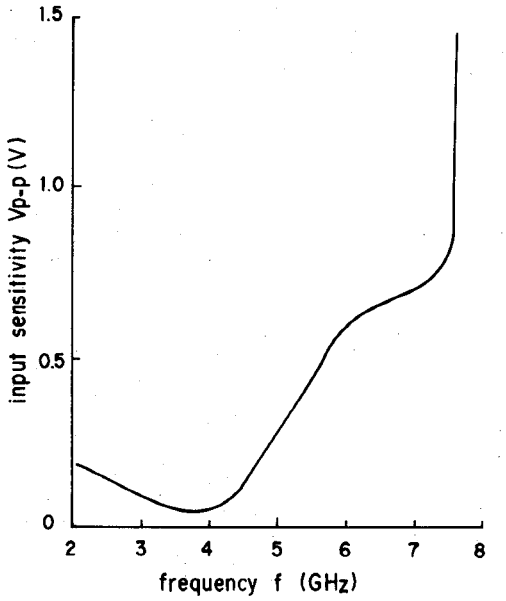


Fig. 4. Input sensitivity $V_{p-p}$ versus operation frequency of the fabricated 1/64 prescaler.

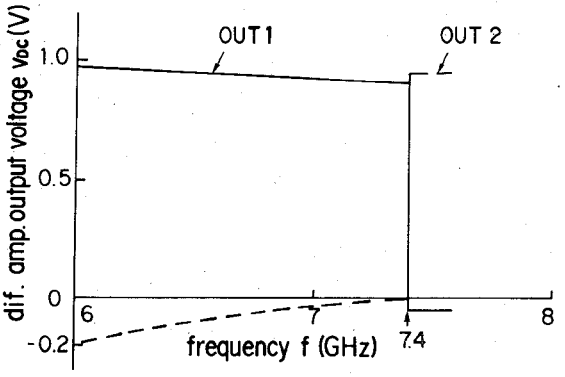


Fig. 5. Overall frequency comparison characteristics of the fabricated prescaler/PFC MSI circuit.

## III. IC Fabrication

The fabrication technology was 0.5-$\mu$m-gate BP-SAINT, starting with 3-in indium-doped LEC crystals. An ion-implantation energy of 30 keV and a dose of $5\times10^{12}$ cm$^{-2}$ were used to form a shallow active layer. The average $V_{th}$ and $g_m$ across a wafer were 0.068 V and 220 mS/mm, respectively. A microphotograph of the fabricated MSI chip with dimensions 3.2 mm$\times$1.2 mm is shown in Fig. 3.

## IV. Performance

The prescaler/PFC MSI circuit was mounted on a newly developed high-frequency package, and the characteristics of the prescaler and the PFC were measured. The high-frequency package was constructed with 50-Ω strip lines and 50-Ω internal matching resistors. The input sensitivity $V_{p-p}$ versus operating frequency of the 1/64 prescaler is shown in Fig. 4. A maximum operating frequency of 7.6 GHz was obtained. For all frequencies up to 7.6 GHz, the prescaler monitor output signal swing into a 50-Ω load was 0.8 V (ECL compatible). The input sensitivity at 7.5 GHz was 0.8 $V_{p-p}$. In determining the overall frequency comparison characteristics of the 1/64 prescaler/PFC MSI circuit, the PFC V input reference frequency was fixed at 115.625 MHz ( = 7.4 GHz/64), the prescaler input frequency was varied from 6.0 to 7.6 GHz, and the two dc output voltages of the differential amplifier were measured. A typical frequency comparison performance is shown in Fig. 5. Output dc voltages changed abruptly at the prescaler input frequency of 7.4 GHz. Total power consumption was 730 mW. The phase noise of the 1/64 prescaler output signal was confirmed to be suppressed until it reached the measurement limit of the HP Model 8566B spectrum analyzer, namely $-85$ dBc.

## V. Conclusions

A high-speed, low-power prescaler/PFC MSI circuit for a phase-locked stable oscillator in satellite and microwave communication systems was designed and fabricated using GaAs MESFET LSCFL circuitry. The fabricated prescaler/PFC MSI circuit, which was mounted on a newly developed high-frequency package, operated up to 7.6 GHz with a power dissipation of 730 mW. It has been determined that this prescaler/PFC MSI circuit is suitable for practical use in satellite and microwave communication systems.

## Acknowledgment

The authors with to thank the members of the processing group for the fabrication process. They would also like to thank M. Idda for offering a package and Dr. T. Sugeta for his constant encouragement.

## References

[1] K. Osafune and K. Ohwada, "Ultra-high-speed GaAs monolithic prescaler and phase frequency comparator IC," *IEEE Trans. Microwave Theory Tech.*, vol. MTT-34, pp. 786–790, July 1986.

[2] T. Takada, Y. Shimazu, K. Yamasaki, M. Togashi, K. Hoshikawa, and M. Idda, "A 2Gb/s throughput GaAs digital time switch LSI using LSCFL," *IEEE Trans. Microwave Theory Tech.*, vol. MTT-33, pp. 1579–1584, Dec. 1985.

[3] K. Yamasaki, N. Kato, and M. Hirayama, "Below 10 ps/gate operation with buried p-layer SAINT FET's," *Electron. Lett.*, vol. 20, nos. 25/26, pp. 1029–1031, 1984.

[4] M. Ida, T. Takada, and M. Ino, "Packages for ultra high speed integrated circuits," in *1986 Nat. Conf. Rec. Optical Radiowave Electron.*, (IECE Japan), p. 138.

[5] T. Takada, K. Yokoyama, M. Idda, and T. Sudo, "A MESFET variable-capacitance model for GaAs integrated circuit simulation," *IEEE Trans. Microwave Theory Tech.*, vol. MTT-30, pp. 719–724, May 1982.

# Application of a Projection Method to a Mode-Matching Solution for Microstrip Lines with Finite Metallization Thickness

FRANK BÖGELSACK AND INGO WOLFF, SENIOR MEMBER, IEEE

***Abstract*—It will be demonstrated that the convergence behavior of the well-known mode-matching technique can be improved significantly by a general projection method. The advantage of this approach becomes obvious in the discussion of the electromagnetic field distribution near metal edges. The implementation is rather simple and will be described below. Numerical results and the validity of this method are discussed for shielded microstrip lines with finite metallization thickness.**

Manuscript received December 30, 1986; revised May 27, 1987.

The authors are with the Department of Electrical Engineering, University of Duisburg, D-4100 Duisburg, West Germany.

IEEE Log Number 8716173.

## I. Introduction

The conventional mode-matching technique (MMT) is a very general tool in the numerical computation of electromagnetic field problems. Contrary to those methods which are problem oriented and optimized, the efficiency of this method is not very high. Nevertheless, because the treatment of two- or three-dimensional field problems requires a full-wave analysis based on a general, rigorous method, this method is often used. To make it more efficient, some modifications are necessary.

The MMT makes use of a subdivision of the field area. The electromagnetic field in each part is expanded into series of corresponding eigenfunctions; the unknown amplitude coefficients of the expansions are determined using the continuity conditions at the interfaces between the different regions. As a result, other specific aspects of the problem cannot be considered additionally by a proper choice of the expansion functions. For example, in the case of a shielded microstrip line with finite metallization thickness, problems arise in the accurate description of the electromagnetic field near the metal strip edges. Care has to be taken in the treatment of the field singularities at the edges.

Although the asymptotic behavior of the field quantities has been described in a fundamental investigation by Meixner [3], [4], the classical MMT does not offer any way to consider these results. To solve this problem, the new treatment described here makes use of a suitable projection method, which drastically reduces the computation time and storage requirements.

## II. Theoretical Approach

Following Kowalski and Pregla [2], the computation of microstrip parameters using MMT can be based on the subdivision shown in Fig. 1.

Eigenfunctions are chosen in such a way that the homogeneous boundary conditions on both the metal strip and the metal shielding are explicitly satisfied by the eigenfunctions of the different regions. The boundary conditions between the different subregions are satisfied as described above. This formulation is capable of predicting such frequency-dependent microstrip parameters as the effective dielectric constant $\epsilon_{\text{eff}}$ and the characteristic impedance $Z_0$. As has been pointed out before, the situation is completely different in the case of calculating the electromagnetic field distribution. It is not possible to describe the field singularities exactly using a finite number of eigenmodes. Because the rank of the resulting matrix is correlated to the number of expansion functions, an exact field description leads to time-consuming numerical computations.

The projection of the tangential electromagnetic field in the interface sections on a new suitable function system $(f_i)$ decouples the rank of the system matrix from the truncation index of the series expansion [1]. These expansion functions $f_i$ are chosen to conform with the assumed field distribution in the region of interest. In the case of the shielded microstrip line, the weighted superposition of all $f_i$ should be able to describe the field singularities at the metal edges.

A simple and complete set of expansion functions is given by a power series. The tangential electric field in the boundary 1–2 (Fig. 1) can be written as

$$E_{1x} = a_0 f_0 + \sum_{i=1}^{M-1} a_i f_i = E_{2x} \tag{1}$$

$$E_{1z} = b_0 g_0 + \sum_{i=1}^{M-1} b_i g_i = E_{2z} \tag{2}$$

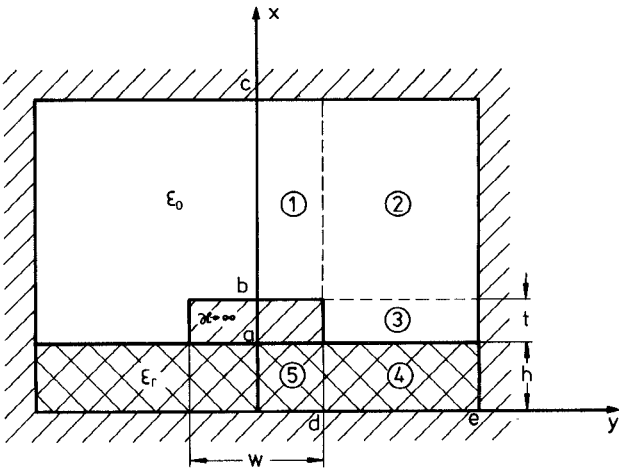


Fig. 1. The microstrip configuration and the subdivision of the cross-sectional field regions.

where

$$f_i = g_i = \left(\frac{x-b}{c-b}\right)^{i-1}.$$

Because of the edge behavior of the $x$ components of the electric field, the power series are extended by an additional term:

$$f_0 = \left(\frac{x-b}{c-b}\right)^{\tau-1}$$

$$g_0 = \left(\frac{x-b}{c-b}\right)^{\tau}$$

where $\tau = \frac{2}{3}$ for the 270° edge [3], [4], [6]. The exponent for the lower edge on the dielectric substrate material (regions 3, 4, 5) is given in [6] by

$$\tau = \frac{2}{\pi} \arctan \sqrt{1 + \frac{2}{\epsilon_r}}. \tag{3}$$

Using the orthogonality of the eigenfunctions in their intervals, the 16 continuity equations of the four boundaries lead to the expansion coefficients of the electromagnetic fields depending on the coefficients $a_i$ and $b_i$ of the power series according to (e.g. for region 1):

$$\langle E_{1x}, e_{1x} \rangle = \langle a_0 f_0, e_{1x} \rangle + \left\langle \sum_{i=1}^{M-1} a_i f_i, e_{1x} \right\rangle \tag{4}$$

$$\langle E_{1z}, e_{1z} \rangle = \langle b_0 g_0, e_{1z} \rangle + \left\langle \sum_{i=1}^{M-1} b_i g_i, e_{1z} \right\rangle \tag{5}$$

where $e_{1x}$ and $e_{1z}$ are the eigenfunctions of region 1. To reduce the numerical expense, a fast Fourier transform is applied for the evaluation of the first term on the right-hand side of (4) and (5).

Substituting the coefficients into the magnetic field components, testing with the power series, and matching these components at the boundaries lead to a set of homogeneous equations

$$A(k_z) K = 0. \tag{6}$$

The rank of the system matrix $A$ is $Rk(A) = 8M$. $K$ is the coefficient vector of the power series, and $k_z$ is the propagation constant of the modes propagating on the microstrip line. The coefficients will be determined by, for example, a Gauss procedure recursively if $k_z$ is known.

TABLE I
GEOMETRICAL AND ELECTRICAL PARAMETERS OF SEVEN MICROSTRIP CONFIGURATIONS AT A FREQUENCY $f = 10$ GHz

| Config. | $\varepsilon_r$ | 2e/mm | c/mm | t/mm | w=2d/mm | h=a/mm | $\left(\frac{k_z}{k_0}\right)^2$ |
|---|---|---|---|---|---|---|---|
| 1 | 2.3 | 3 | 2 | 0.0175 | 1.0 | 0.635 | 1.76 |
| 2 | 10.0 | 3 | 2 | 0.0175 | 1.0 | 0.635 | 6.59 |
| 3 | 2.3 | 12 | 8 | 0.0175 | 1.0 | 0.635 | 1.88 |
| 4 | 10.0 | 12 | 8 | 0.0175 | 1.0 | 0.635 | 7.35 |
| 5 | 2.3 | 12 | 8 | 1.0 | 1.0 | 0.635 | 1.74 |
| 6 | 10.0 | 12 | 8 | 1.0 | 1.0 | 0.635 | 6.50 |
| 7 | 12.8 | 0.6 | 0.4 | 0.005 | 0.005 | 0.100 | 6.4 |

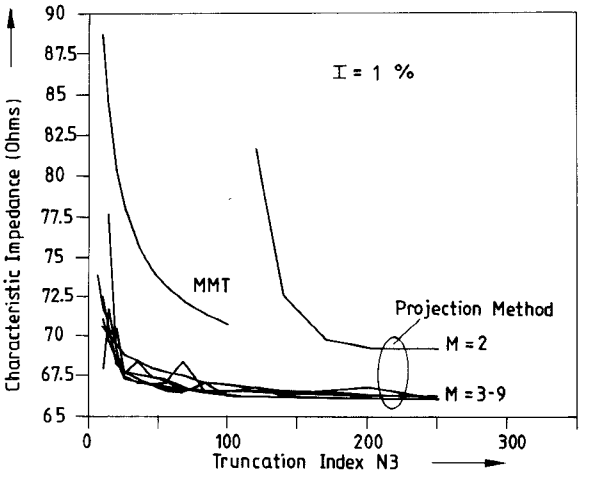


Fig. 2. The characteristic impedance of configuration 1 as a function of the truncation index $N3$ of the vector potentials and with the truncation index $M$ of the power series as a parameter, calculated by the MMT and the projection method.

## III. EXAMPLES

To demonstrate the advantage of the projection method described above, calculations of microstrip characteristic impedance have been performed.

Table I shows the geometrical and electrical parameters of six different microstrip lines with $w = 2d = 1$ mm, $h = a = 0.635$ mm, and frequency $f = 10$ GHz.

The characteristic impedance is given by

$$Z_0 = Z_{PI} = 2\frac{P_z}{I_z^2} \tag{7}$$

where

$$P_z = \frac{1}{2}\,\mathrm{Re}\left\{ \iint_A (\vec{E} \times \vec{H}^*)\, dA \right\}_z$$

is the power transported by the wave.

It is possible to introduce three different truncation indices, $N_1$, $N_3$, and $N_5$, for regions 1, 3, and 5, respectively. The number of amplitude coefficients of the field expansions for the regions 2 and 4 are determined by the truncation indices of the neighboring regions.

There are no physical reasons for introducing any ratio of the three indices, because the relative convergence phenomenon does not occur. Therefore the calculations by the MMT are investigated with $N_1 = N_3 = N_5$. On the other hand, it leads to numerical advantages if the series are truncated corresponding to the geometries of the orthogonal intervals:

$$N_1 : N_3 : N_5 = (c - b) : (e - d) : a.$$

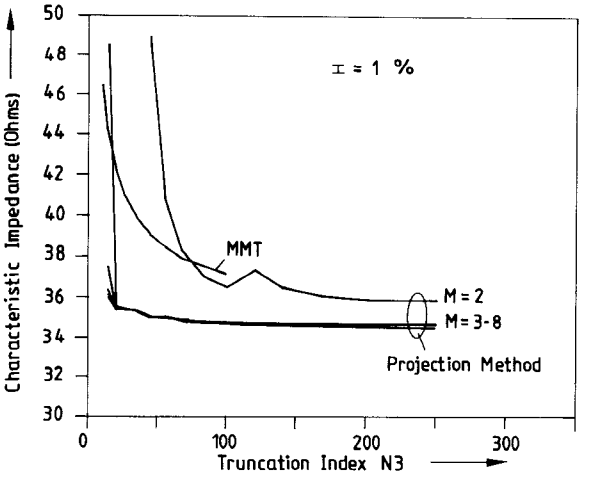


Fig. 3. The characteristic impedance of configuration 2 as a function of the truncation index $N3$ of the vector potentials and with the truncation index $M$ of the power series as a parameter, calculated by the MMT and the projection method

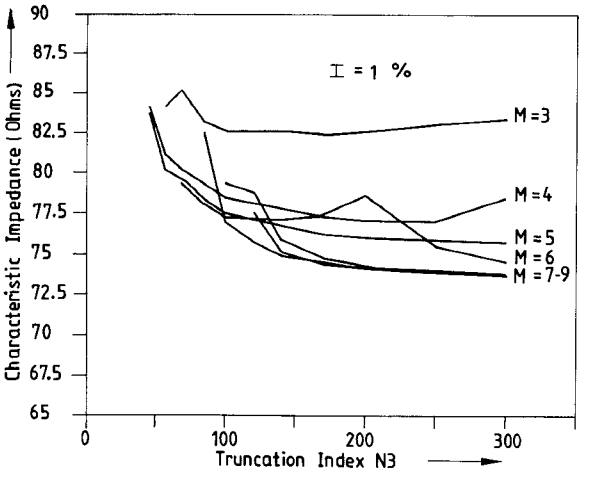


Fig. 4. The characteristic impedance of configuration 3 as a function of the truncation index $N3$ of the vector potentials and with the truncation index $M$ of the power series as a parameter, calculated by the projection method.

Figs. 2–6 show the computed characteristic impedances as a function of $N_3$, calculated by the MMT and the projection method. $M$ is the truncation index of the power series. The 1-percent error bar is related to the mean value of the impedances, shown on the ordinate.

Comparing the two methods with respect to convergence (Figs. 2–5), the projection method yields more accurate results for a given truncation index $M > 2$. Additionally, the decoupling of the rank of the system matrix from the truncation indices $N_1$, $N_3$, and $N_5$ makes it possible to consider more coefficients of the vector potentials to improve the field description near the metallization edges. The power of the projection method against the MMT is shown in the case of configuration 3 (large shielding dimensions). Here the MMT does not deliver a solution within the range shown in Fig. 4, whereas the projection method shows good convergence for truncation indices $M > 6$.

The improvement given by the projection method can be explained as follows: In the case of the MMT the electromagnetic field along the boundaries is adjusted in such a way that the mean quadratic error is nearly equal over the total considered intervals. The power series of the projection method which consider the edge behavior of the field result in a weighting of the

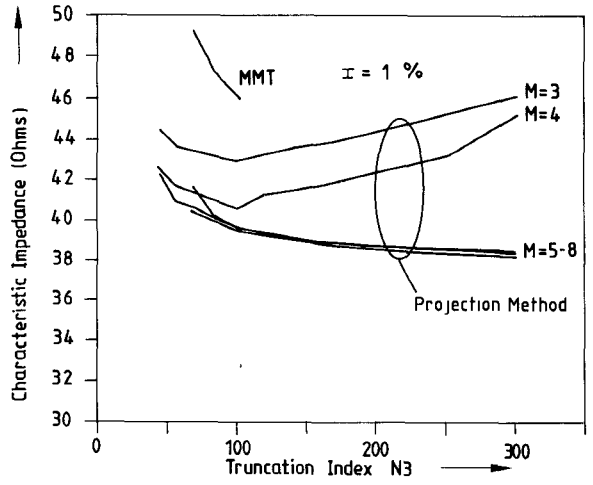


Fig. 5. The characteristic impedance of configuration 4 as a function of the truncation index $N3$ of the vector potentials and with the truncation index $M$ of the power series as a parameter, calculated by the projection method.

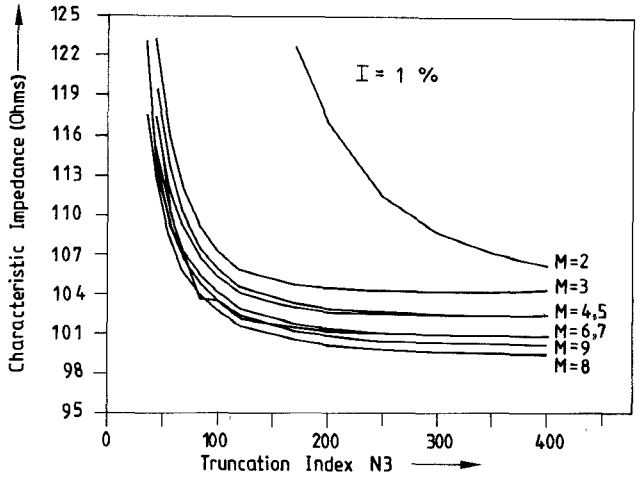


Fig. 6. The characteristic impedance of configuration 7 as a function of the truncation index $N3$ of the vector potentials and with the truncation index $M$ of the power series as a parameter, calculated by the projection method.

error near the edge, so that the electromagnetic field (using the same truncation indices) is approximated much better by the projection method than by the MMT.

For very large metallization thicknesses (configurations 5 and 6: $t = 1$ mm, nearly twice the substrate height), both the projection method and the MMT fail. Considering a more realistic configuration, for example, a quadratic metal strip on a GaAs substrate of the type used in monolithic microstrip integrated circuits (MMIC) (configuration 7: $\epsilon_r = 12.8$, $2e = 600\ \mu$m, $c = 400\ \mu$m, $t = w = 2d = 5\ \mu$m, $h = a = 100\ \mu$m, $f = 10$ GHz, $(k_z/k_0)^2 = 6.4$), a good convergence behavior is obtained, whereas the conventional MMT delivers no results again within the ordinate range (Fig. 6). Using the projection method, numerical problems occur for a truncation index $M = 10$.

## IV. Conclusions

The application of a projection method, based on an idea by Jansen [1], delivers good results for the characteristic impedance of microstrip configurations with finite metallization thickness. It should be emphasized that the procedure of the projection method is a general one which can be applied to various boundary value problems.

## Acknowledgment

The diligent support of Mr. S. Koßlowski and many helpful discussions with Dr. P. Waldow are thankfully acknowledged.

## References

[1] R. H. Jansen, *Lectures on Computer-Oriented Field Theory*. Universität Duisburg, West Germany, 1980.
[2] G. Kowalski and R. Pregla, "Dispersion characteristics of shielded microstrips with finite thickness," *Arch. Elek. Übertragung.*, vol. 25, no. 4, pp. 193–196, 1971.
[3] J Meixner, "The behavior of electromagnetic fields at edges," *IEEE Trans. Antennas Propagat.*, vol. AP-20, pp. 442–446, 1972.
[4] J. Meixner, "Die Kantenbedingung in der Theorie der Beugung elektromagnetischer Wellen an vollkommen leitenden ebenen Schirmen," *Ann. Phys.*, vol. 6, pp. 2–9, 1949.
[5] C. Vassallo, "On a direct use of edge conditions in modal analysis," *IEEE Trans Microwave Theory Tech.*, vol. MTT-24, pp. 208–212, Apr. 1976.
[6] R. Mittra and S. W. Lee, *Analytical Techniques in the Theory of Guided Waves* New York: Macmillan, 1971.

# Parametric Equations for Surface Waves in Dielectric Slab

JEFFREY C. HANTGAN, MEMBER, IEEE

***Abstract*—For the dielectric slab it is shown that 1) the dispersion curve for the $n$th surface wave can be found using parametric equations in which the normalized inside wavenumber $K_{x1}$ and the mode number are the parameters, 2) the dispersion curve for the $n$th surface wave mode can also be found by using parametric equations in which the mode number and a modified wavenumber $x'$ with common domain $[0, \pi/2]$ are the parameters, and 3) all TE or all TM dispersion curves for surface waves are related to each other by a simple algebraic equation using the mode numbers and the normalized propagation constants $K_0$ and $\beta$ as the variables.**

## I. Fundamental Equations

Presently, dispersion curves for surface waves in dielectric slab are obtained using either a graphical or a computer technique [1], [2]. These techniques are unnecessary since the dispersion curves can be obtained much more easily using parametric equations. In addition, these graphical or computer techniques obscure the simple algebraic relation between two different TE or two different TM surface waves. This simple algebraic relation can be used to express the $m$th surface wave in terms of the $n$th surface wave propagation constants.

The normalized dispersion equations (normalized w.r.t. the slab width $2d$) for surface waves in dielectric slab are

$$K_{x1} \tan K_{x1} = \delta K_{x2} \qquad \text{(symmetric modes)} \quad (1a)$$

$$K_{x1} \operatorname{ctn} K_{x1} = -\delta K_{x2} \qquad \text{(antisymmetric modes)} \quad (1b)$$

where $\delta = 1$ for TE modes, or $\delta = \epsilon_r/\epsilon_0$ (the ratio of the relative permittivities) for TM modes [1]–[3]. Since the value of $K_{x2}$ must be positive, $K_{x1}$ lies in the range

$$n\frac{\pi}{2} \leq K_{x1} \leq (n+1)\frac{\pi}{2} \qquad n = 0,1,2,\cdots \quad (2)$$

Manuscript received January 23, 1987; revised June 1, 1987.
The author is with the Department of Electrical Engineering, State University of New York at Stony Brook, Stony Brook, NY 11794-2350.
IEEE Log Number 8716174.